

RESEARCH

Open Access



# Identification of functional pathways and molecular signatures in neuroendocrine neoplasms by multi-omics analysis

Viola Melone<sup>1†</sup>, Annamaria Salvati<sup>1,2†</sup>, Domenico Palumbo<sup>1</sup>, Giorgio Giurato<sup>1,2,3</sup>, Giovanni Nassa<sup>1,2,3</sup>, Francesca Rizzo<sup>1,2,3</sup>, Luigi Palo<sup>1</sup>, Alessandro Giordano<sup>1</sup>, Mariarosaria Incoronato<sup>4</sup>, Mario Vitale<sup>5</sup>, Caterina Mian<sup>6</sup>, Immacolata Di Biase<sup>7</sup>, Stefano Cristiano<sup>7</sup>, Viviana Narciso<sup>7</sup>, Monica Cantile<sup>8</sup>, Annabella Di Mauro<sup>8</sup>, Fabiana Tatangelo<sup>8</sup>, Salvatore Tafuto<sup>9</sup>, Roberta Modica<sup>10</sup>, Claudia Pivonello<sup>10</sup>, Marco Salvatore<sup>4</sup>, Annamaria Colao<sup>10,11</sup>, Alessandro Weisz<sup>1,2,3\*</sup> and Roberta Tarallo<sup>1,2,3\*</sup> 

## Abstract

**Background:** Neuroendocrine neoplasms (NENs) represent a heterogeneous class of rare tumors with increasing incidence. They are characterized by the ability to secrete peptide hormones and biogenic amines but other reliable biomarkers are lacking, making diagnosis and identification of the primary site very challenging. While in some NENs, such as the pancreatic ones, next generation sequencing technologies allowed the identification of new molecular hallmarks, our knowledge of the molecular profile of NENs from other anatomical sites is still poor.

**Methods:** Starting from the concept that NENs from different organs may be clinically and genetically correlated, we applied a multi-omics approach by combining multigene panel testing, CGH-array, transcriptome and miRNome profiling and computational analyses, with the aim to highlight common molecular and functional signatures of gastroenteropancreatic (GEP)-NENs and medullary thyroid carcinomas (MTCs) that could aid diagnosis, prognosis and therapy.

**Results:** By comparing genomic and transcriptional profiles, ATM-dependent signaling emerged among the most significant pathways at multiple levels, involving gene variations and miRNA-mediated regulation, thus representing a novel putative druggable pathway in these cancer types. Moreover, a set of circulating miRNAs was also selected as possible diagnostic/prognostic biomarkers useful for clinical management of NENs.

**Conclusions:** These findings depict a complex molecular and functional landscape of NENs, shedding light on novel therapeutic targets and disease biomarkers to be exploited.

**Keywords:** Neuroendocrine neoplasms, Molecular signatures, ATM signaling, Circulating biomarkers

## Introduction

Neuroendocrine neoplasms (NENs) are a class of rare and heterogeneous tumors whose molecular pathogenesis is an open issue. NENs are characterized by a body-wide distribution because they develop from neuroendocrine system cells, which are spread throughout the whole body [1–3]; they mainly arise in gastrointestinal and pulmonary tract, but can also arise from thyroid,

<sup>†</sup>Viola Melone and Annamaria Salvati contributed equally to this work

\*Correspondence: [aweis@unisa.it](mailto:aweis@unisa.it); [rtarallo@unisa.it](mailto:rtarallo@unisa.it)

<sup>1</sup> Laboratory of Molecular Medicine and Genomics, Department of Medicine, Surgery and Dentistry “Scuola Medica Salernitana”, University of Salerno, via S. Allende, 84081 Baronissi, SA, Italy  
Full list of author information is available at the end of the article



pituitary gland, lung, breast or larynx or other organs and tissues [4]. These neoplasms can occur both in sporadic form and in hereditary syndromes such as multiple endocrine neoplasia type 1 and 2 (MEN1 and MEN2), von Hippel–Lindau disease (VHL), neurofibromatosis type 1 (NF1) and the tuberous sclerosis complex (TSC) [5, 6].

NENs originating from pancreas and the gastro-intestinal tract, the gastroenteropancreatic NENs (GEP-NENs) are among the most common forms. The World Health Organization (WHO) and the International Agency for Research on Cancer (IARC) classified GEP-NENs based on tumor primary sites and on the morphological differentiation features by which these neoplasms can be divided into the well-differentiated tumors (NETs) and poorly-differentiated carcinomas (NECs) [4]. According to proliferation index and mitotic count, GEP-NENs have been categorized into low (G1, Ki67 < 3%), intermediate (G2, Ki67 3–20%) and high (G3, Ki67 > 20%) grades [7]. Particularly, NET comprised well differentiated tumors with G1, G2 and G3 grade, while NEC comprised poorly differentiated carcinomas with G3 grade [7].

The thyroid NENs are tumors of parafollicular C-cells that are conventionally known as medullary thyroid carcinomas (MTCs) [8]; they represent 3–5% of all thyroid carcinomas and can develop, in ~30% of the cases, in the context of MEN2 syndromes [9]. In MTCs the Ki-67 index, conventionally used for GEP-NENs classification, is difficult to assess, being often lower than 1%, so a classification based on this parameter is not currently used [4].

Specific genomic profiles and genetic signatures have been previously observed among GEP-NENs with different primary sites and degrees of differentiation and in MTCs, with pancreatic NENs being the best described in the literature. In pancreatic NETs, somatic mutations in MEN1, DAXX, ATRX, PTEN, TSC2 and members of the mTOR signaling pathway were observed [10–12]. Moreover, sporadic pancreatic NETs also present germline mutations in the DNA repair genes MUTYH, CHEK2 and BRCA2 [11]. On the other hand, gastrointestinal NETs (GI-NETs) frequently show mutations in CDKN1B gene [13, 14]. In contrast, both pancreatic and intestinal NECs commonly show mutations in TP53 and RB1 and may share mutations in KRAS and SMAD4 [13, 15, 16]. In MTCs mutations in RET gene were described, affecting tumor microenvironment and angiogenesis, and this has been linked to poor prognosis compared to MTCs that are RAS mutated [4, 17]. Overall, from the genomic point of view, the loss of chromosome 18 has been reported in small bowel NETs, even if the biological significance of this alteration is still unknown [18]. However, in pancreatic NETs, the loss of genetic material has been described more often than chromosomal gains [11].

Generally, NENs are characterized by a relatively indolent rate of growth and by the ability to secrete peptide hormones and biogenic amines that are used as biomarkers [18]. However, over the latest 40 years the incidence and the prevalence of these tumors have increased more than sixfold in the United States [19] and, due to non-specific symptomatology and lack of early markers, many NENs show metastatic profile at diagnosis, making it sometimes impossible to identify the primary site of tumor lesion [3, 20, 21].

A further problem, in addition to a more accurate classification, is the lack of specific markers for NEN diagnosis; Chromogranin A (CgA), synaptophysin (Syn), 5-Hydroxyindoleacetic Acid (5-HIAA), neuron-specific enolase (NSE) and cluster of differentiation 56 (CD56) (neural cell adhesion molecule) are currently used for GEP-NENs diagnosis [18, 22] and Calcitonin for MTCs [23]. In GEP-NENs, both Syn and CgA are highly expressed in well-differentiated neoplasms, whereas poorly differentiated carcinomas often maintain synaptophysin positivity while losing CgA expression and acquiring NSE expression [18]. CgA is characterized by low sensitivity and specificity and the tests can give lots of false-positive elevations [24, 25]. Equally, the prognostic role of 5-HIAA remains controversial [26]. For MTC diagnosis, calcitonin is a sensitive tumor marker because it correlates with C-cell mass and burden of the neoplasms [23], but this has also some limitations, such as inter-assay variability, concentration-dependent half-life and rapid degradation [23].

To meet this clinical need, in our study we aimed to identify novel prognostic factors and biomarkers for the improvement of the histologic and pathologic evaluation of NENs which is a key component of clinical management [27, 28]. Particularly, our attention was focused on genome, transcriptome and miRNome profiles of tumor biopsies through a multi-omics approach. The case cohort studied included 66 specimens from GEP-NENs at different grades and MTCs. In few cases only metastatic tissues were available, mainly among neoplasms with gastroenteropancreatic primary location, and these were analyzed as a separate group. Moreover, in order to link our results to clinical management, serum samples of NENs patients were analyzed to determine presence and concentration in the serum of NEN patients of the miRNAs highly expressed within the corresponding tumor tissue. This study design allowed the identification of a subset of molecules able to discriminate healthy from sick subjects, as well as to find some miRNAs significantly correlating with clinical-pathologic features of the neoplasms. These might have a strong impact for diagnostic and

prognostic purposes respectively, as therapeutic sequence in patients with NENs is still debated [29, 30].

Moreover, altogether the obtained results revealed the ataxia telangiectasia mutated (ATM) signaling among the most significantly impacted at different levels, considering gene variants as mutations and amplifications and miRNA expression deregulation. Indeed, this might represent a putative targetable pathway in the treatment of NENs.

## Subjects and methods

### Patients characteristics and pathological assessment

Tumor biopsies from 46 NEN patients (Thyroid n=17, Pancreas n=14, Intestine n=12 and Lung n=3) were collected by the biobank of the “Istituto Nazionale Tumori-IRCCS-Fondazione G. Pascale” (Naples, Italy) and by the Department of Clinical Medicine and Surgery, Endocrinology Unit of Federico II University (Naples, Italy). Out of 46 tumor tissues, 19 were FFPE sections (Formalin fixed paraffin embedded) while 27 were frozen sections. In addition, a validation set of 20 previously isolated RNAs from MTCs were obtained from Endocrinology Unit, Department of Medicine (DIMED), University of Padua. Patient characteristics and samples pathology were summarized in Table 1.

Cases have been reviewed by an expert pathologist (FT) and graded and staged according to WHO 2017 and 2019 classification criteria (NET-G1, NET-G2, NET-G3, NEC-G3) on tissue sections. The 4 main categories are distinguished on the basis of the proliferative activity, measured through the mitotic count and the Ki67 expression. In our cohort, high-grade (G3) specimen were all classified as poorly differentiated according to Hematoxylin/Eosin staining, thus they all fall within NECs. Medical records have been reviewed for clinical information, including histologic parameters, assessed on standard H&E-stained slides combined with immunohistochemical staining with neuroendocrine markers, and tumor location. Immunohistochemical staining for Ki67 (clone MM1, Leica), Chromogranin A (clone 5H7, Leica, Wetzlar, Germany, ready to use), Synaptophysin (clone 27G12, Leica, ready to use) and Calcitonin (clone CL1948, Leica, ready to use) has been performed using the En Vision method (DAKO, Denmark) following the manufacturer's instruction.

For miRNA validation in liquid biopsies, serum from 42 NEN patients (6 MTCs and 36 GEP-NENs) and 34 healthy subjects were obtained.

### Nucleic acids extraction

DNA and RNA isolations were performed from both FFPE and frozen sections using FFPE DNA Purification Kit (Cat. 47400, Norgen Biotek Corp, Thorold, Canada)

**Table 1** Patients' clinical data

Classification	Number/percentage (n = 66)
Gender	
Male	33 (50%)
Female	33 (50%)
Tumor location	
Thyroid	37 (56.1%)
Pancreas	14 (21.2%)
Intestine	12 (18.2%)
Lung	3 (4.5%)
Metastases	19 (28.8%)
Grading classification (WHO 2019) for p-NET, I-NET and lung-NET	
NET G1 (Ki-67% ≤ 2)	11 (38%)
NET G2 (Ki-67% 3–20)	11 (38%)
NEC G3 (Ki-67% > 20)	7 (24%)
Genetic syndrome	
Men1	1 (2%)
Men2	3 (7%)
ND	1 (2%)
Status	
Live	53 (80.3%)
Dead	7 (10.6%)
nd/progression	6 (9.1%)

and RNA/DNA Purification Kit (Cat. 48700, Norgen Biotek Corp.) respectively, according to the manufacturers protocol. Nucleic acids were quantified with Qubit 2.0 fluorometer using Qubit RNA HS assay kit and Qubit DNA HS assay kit (Thermo Fisher Scientific, Waltham, Massachusetts, USA). The assessment of nucleic acids integrity (DIN and RIN) was performed with Agilent 4150 TapeStation System (Agilent Technologies, Santa Clara, CA, USA).

### Mutational profiling

Libraries for mutational profiling were prepared, starting from 40 ng of DNA as input material, with TruSight™ Oncology500 kit (Cat. 20028213, Illumina, San Diego, California, USA) according to manufacturer's protocol. These consist in a targeted-capture of 523 cancer-relevant genes. The libraries were sequenced on NextSeq 500 (Illumina) in 2 × 150 bp or 2 × 75 bp in paired end mode. Sequencing data were analyzed using the TruSight Oncology 500 Local App Version 2.2 (Illumina) to identify variants, gene amplifications, TMB and MSI. The genomic coordinates of all the identified variants were subsequently converted to hg38 using LiftOver [31].

Variants were annotated with Annovar [32]. Those with coverage depth lower than 100 and variants occurring

with a frequency higher than 5% in 1000G or GnomAD were discarded. The sequence variants annotated as “benign” or “likely benign” in ClinVar database were also filtered out. Furthermore, variants classified as synonymous or in intergenic positions were discarded. Onco-plots were generated using Maftools [33] on R (v4.0.2). Functional analysis was performed using Ingenuity Pathway Analysis (IPA, Qiagen, Hilden, Germany) and only the pathways with more than 1.3 in  $-\log$  of the adjusted p-value were considered.

#### Array-CGH

Array-CGH analysis was performed using Agilent Oligonucleotide Array-Based CGH for Genomic DNA Analysis-Enzymatic Labeling (Agilent Technologies, Santa Clara, CA, USA), starting from 500 ng of DNA, following the manufacturer’s instructions. The microarray includes 60,000 oligonucleotide probes. Genomic DNA samples and reference samples were labeled with Cy5 and Cy3, respectively, using the SureTag DNA Labeling Kit and following Agilent Enzymatic Labeling protocol. Labeled genomic DNA was purified using the reaction Purification Column provided with the kit. After the hybridization protocol, slides were scanned using Agilent SureScan Dx Microarray Scanner G5761A. Image files were analyzed using Agilent Cytogenomics 5.0.0.38 Software, and genomic coordinates were evaluated according to GRCh38/hg38. The measure of success of profiling for each sample was based on array data sample quality indices (derivative log ratio scores). Circos plot was generated using circos (v0.69.9) [34].

#### Transcriptome profiling

Libraries preparation for transcriptome analysis was performed employing the TruSeq RNA Exome kit (Cat. 20020189, Illumina) for FFPE samples and TruSeq Stranded Total RNA kit (Cat. 20020598, Illumina) for frozen samples, starting from 200 and 400 ng of RNA as input materials, respectively, according to manufacturers’ guidelines. 46 libraries were sequenced on NextSeq 500 (Illumina) using  $2 \times 75$ pb paired end and 14 libraries on HiSeq 1500 (Illumina) using  $1 \times 50$  single read.

Raw reads were pre-processed using FastQC software [35] to evaluate raw sequences quality and adapter sequences were removed using cutadapt (v3.3) [36]. Alignment was performed on human genome version hg38 (release 34) with STAR (v2.7.8a) [37] and expressed transcripts were identified using featureCounts on Rsubread (v2.0.1) [38]. Differential expression analysis was performed using DESeq2 package (v1.28.1) in R [39], with default parameters. Transcripts were considered differentially expressed if they showed  $|FC| \geq 1.5$  and adjusted p-value  $\leq 0.05$ . Fusion transcripts detection was

performed with STAR-Fusion tool [40], setting default parameters and only fusion transcripts with more than 10 junction reads were considered.

#### Small-RNA profiling

Small-RNA libraries were prepared with NEXTFLEX Small RNA-Seq Kit v3 (Cat NOVA-5132-06, Perkin Elmer, Massachusetts, USA) starting from 50 ng of RNA as input, according to manufacturer’s guidelines. The libraries were sequenced on NextSeq 500 (Illumina) using  $1 \times 75$  bp single read. miRNA-Seq data analysis was performed using the automated pipeline iSmaRT [41]. Target prediction was performed using miRWalk [42]. Only targets validated and present on TargetScan or miRDB with more than 10 reads in at least 60% of the samples were considered. Gene ontology plot was generated using the library GOplot on R [43]. Network was generated using Cytoscape v 3.9.0 [44].

#### Serum sampling, RNA extraction, reverse transcription and real-time PCR

Serum was obtained from whole blood samples by centrifugation at  $1900 \times g$  for 10 min at  $4^\circ\text{C}$ . The supernatant was further centrifuged at  $16,000 \times g$  for 10 min at  $4^\circ\text{C}$  and stored in aliquots of 0.5 ml at  $-80^\circ\text{C}$  until analysis. The extraction of total RNA from 200  $\mu\text{l}$  of serum was performed within 1 year of storage at  $-80^\circ\text{C}$  using miRNeasy Serum/Plasma Kit (Qiagen, Hilden, Germany) according to the manufacturer’s instructions. Briefly, 1  $\mu\text{l}$  of UniSp2 spike-in (Qiagen, Hilden, Germany), a control for the quality of RNA extraction, was combined with the lysis buffer before mixing with the serum. Total RNA (including miRNAs) was eluted in 14  $\mu\text{l}$  of RNase-free water. Reverse transcription was performed using miRCURY LNA™ RT Kit (Qiagen, Hilden, Germany) according to the manufacturer’s instructions. Briefly, 1  $\mu\text{l}$  of UniSp6 spike-in (Qiagen, Hilden, Germany), a control for the quality of RT reaction, was added to the reaction mix including 2  $\mu\text{l}$  of total RNA, nucleic acid mix buffer and reverse transcriptase in a final volume of 10  $\mu\text{l}$ . RT mix was incubated for 60 min at  $42^\circ\text{C}$  and for 5 min at  $95^\circ\text{C}$ . cDNA was stored at  $-20^\circ\text{C}$  until analysis.

Expression value of hsa-mir-106b-3p, hsa-mir-143-3p, hsa-mir-144-3p, hsa-mir-150-5p, hsa-mir-18a-5p, hsa-mir-21-5p, hsa-mir-222-3p, hsa-mir-26a-5p, hsa-mir-335-5p, hsa-mir-361-3p, hsa-mir-375, hsa-mir-7-5p, and hsa-mir-942-5p was determined by real-time PCR using miRCURY LNA miRNA primers (Qiagen, Hilden, Germany) and miRCURY LNA™ SYBR Green PCR Kit (Qiagen, Hilden, Germany), with the instrument CFX384 (Biorad, USA). PCR cycling conditions were  $95^\circ\text{C}$  for 2 min, 40 cycles of  $95^\circ\text{C}$  for 10 s,  $56^\circ\text{C}$  for 60 s and melting curve analysis  $60\text{--}95^\circ\text{C}$ . The maximum cycle threshold (Ct) value was set at 280. UniSp2 and UniSp6 were

used as control genes. Experiments were carried out in triplicates for each data point, and data analysis was done by using CFX Maestro Software (Biorad, USA). Data were expressed as relative expression using the  $2^{-\Delta\Delta Ct}$  method (compared to healthy patients).

## Results

### Samples selection, tissues morphological features and immunostaining

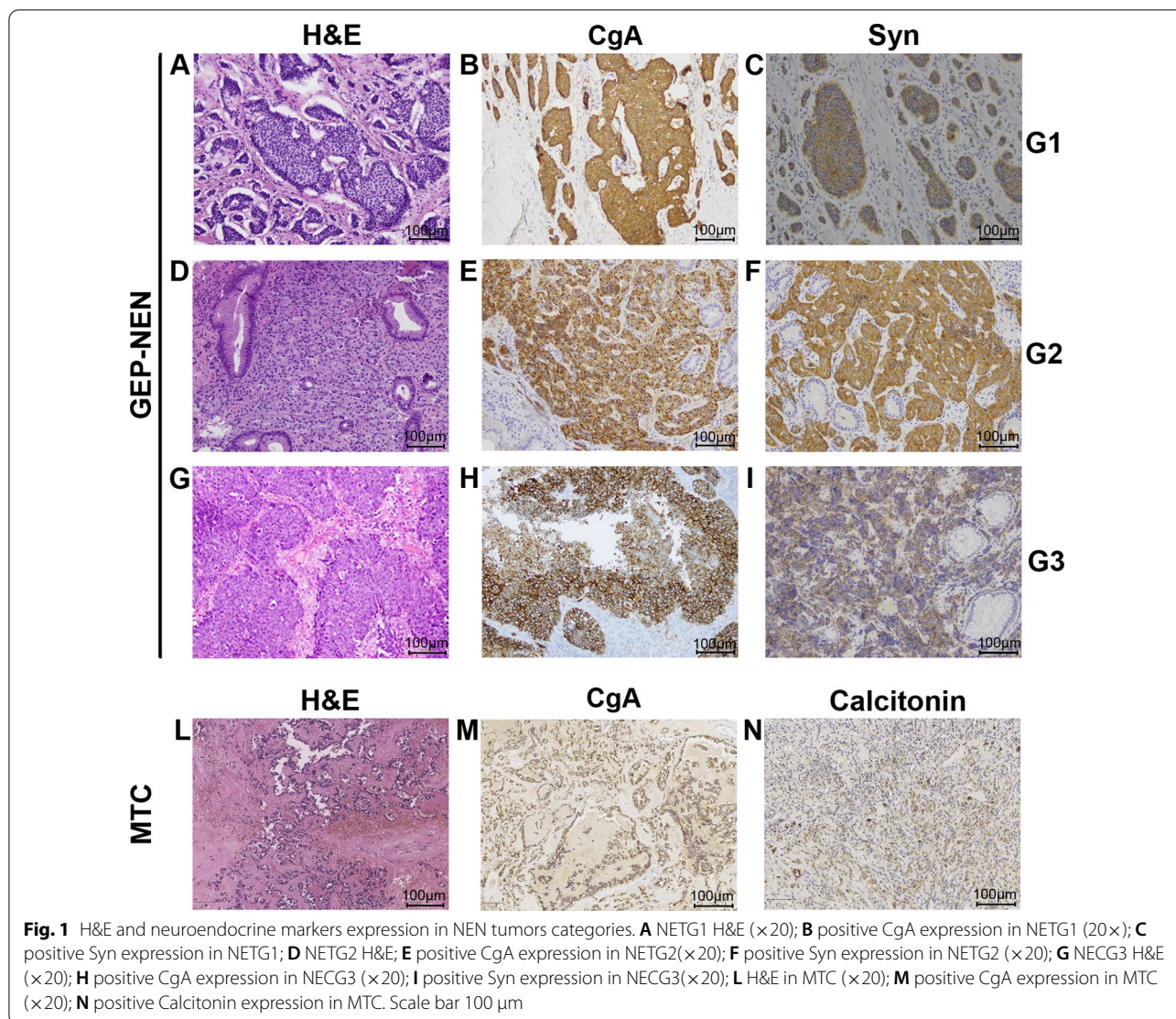
The patients' cohort analyzed in the study was globally composed of 66 samples, including 29 GEP-NENs at different grades and 37 MTCs (Table 1 and Additional file 1: Table S1). Among them, 46 were either frozen tissues or FFPE and were used for the different assays, while 20 previously isolated RNA samples represented a MTC transcriptomics validation set. Moreover, for 5 GEP-NENs, we did not have access to primary tumors, but had instead metastatic tissues (2 hepatic and 3 lymphatic). Clinical and experimental information for each sample were summarized in Additional file 1: Table S1.

We applied a multi-omics experimental approach to identify altered genes, coding transcripts and miRNAs, specifically affecting functional pathways in the investigated NENs.

Where possible, according to the quality and the quantity of the samples available, we performed multigene panel sequencing, RNA-Seq and smallRNA-Seq (Additional file 1: Table S1). For a smaller set (30 samples), we also performed molecular karyotype by comparative genomics hybridization (CGH) array (Additional file 1: Table S1). Samples were classified as G1-G2 GEP-NETs, G3 GEP-NECs and MTCs, according to new histopathological classification, based on tumor grading and cell differentiation (Fig. 1A, D, G, L) [45, 46]. Moreover, we validated the positive staining of CgA and Syn immunohistochemical markers, used in routine histopathological diagnostics, to confirm tumor categories of NENs (Fig. 1B, E, H, C, F, I) [47] and the positive staining of CgA and Calcitonin, specific immunohistochemical markers of MTC (Fig. 1M, N) [48]. In Fig. 1 representative images of the above described morphologic and histopathologic features are shown. Clustering analysis, performed to evaluate possible samples variability emerging when comparing FFPE and fresh/frozen tissues, revealed that our samples were best grouped according to the histotype than to sample storage and library preparation method (data not shown). However, all these sources of variance were taken into account in downstream analyses.

### Assessment of multigene mutational signatures in NENs

DNA isolated from 46 either frozen or FFPE NEN-tissues was analyzed by NGS, to identify genes more likely to be subject to sequence variations among 523 cancer-related ones. After sequencing, two samples were discarded from further analysis due to low quality. In detail, the method allows the simultaneous analysis of multiple biomarkers from different tumor tissues, assessing multiple variant types in a single assay, including small nucleotide variants (SNVs), indels, splice variants and emerging immunotherapy biomarkers such as tumor mutational burden (TMB) and microsatellite instability (MSI). This method has also been recently applied successfully for the identification of genomic features of head and neck neuroendocrine carcinoma [49]. In our case, all the sequence variants identified have been reported in Additional file 2: Table S2. After variants annotation and filtering out of the synonymous variants, the intergenic, those covered less than 100X, those present more than 5% within the general population, and those annotated as "benign" or "likely benign" in ClinVar database, as described in material and methods, we identified 5047 variants. Among them most were intronic, while near 18% were exonic (Fig. 2A); considering only exonic and splicing variants, more than 80% were nonsynonymous SNVs (Fig. 2B). In Fig. 2C are listed the top 20 mutated genes among all NENs examined, considering only exonic and splicing variants. Interestingly, the most frequently mutated gene among all kind of tissues analyzed was the mediator of DNA damage checkpoint protein 1 (MDC1). This is a critical DNA damage response (DDR) effector, acting as anti-apoptotic factor by interacting with TP53, whose loss is generally associated with genomic instability and tumorigenicity [50, 51]. Despite its key role in homologous recombination repair, also including other factors such as ATM and BRCA1 that are among the top mutated genes in the samples analyzed, it has never been found significantly altered in NENs so far, although its role in cancer development and treatment is emerging [52]. Another evidence was that, differently than most of the other genes, MDC1 was mostly affected by multiple variants per sample, a trend that was lesser shared by NUTM1, ZFH3 and FAT1 respectively. Similar behavior was observed in single cases for the remaining, instead missense mutations were most frequently globally observed, while frameshift insertions or deletions and in frame deletions were sporadic events. Then, although we considered altogether all NEN samples, among the top 20 mutated genes NUTM1, ERCC4, MAP3K1, MAP3K4,



RET and RPS6KB2, differently from the other genes, were never mutated in gut tissues but only in thyroid and pancreas deriving tumors (Fig. 2C). On the other hand, taking into account MTCs and GEP-NENs independently (Additional file 3: Fig. S1), we retrieved, within the top mutated genes, already known drivers

and aggressiveness markers, such as HRAS and RET for MTCs (Additional file 3: Fig. S1A), MEN 1 for GEP-NETs (Additional file 3: Fig. S1B), RB1 and TP53 for GEP-NECs (Additional file 3: Fig. S1C).

Functional annotation analysis performed on the globally top mutated genes confirmed, as expected, that

(See figure on next page.)

**Fig. 2** Mutational landscape of 44 NENs. **A** Pie chart showing proportions and genomic localizations of the identified variants after filtering and their **B** exonic function. **C** Oncoplot representation of the TOP 20 mutated genes in the analyzed samples. Only exonic and splicing mutations are represented. Each column represents individual patients with proper numeric code listed lower the graph and mutated genes are listed on the y-axis. The box colors indicate the type of mutation. The upper bar plots represent the total number of exonic/splicing variants identified for each sample within the represented gene set, while the right bar plots indicate the percentage of mutated samples for each gene. Colored bars in the bottom figure depict the pathological features of the patients; the upper is referred to cancer histotype: MTC, Gut, Pancreas and Others (lung-NEN and metastases), the middle indicates the WHO grade for GEP-NENs and the lower is referred to the presence of familiar syndrome. **D** Ingenuity Pathway Analysis (IPA) of the TOP 20 mutated genes. The red line indicates p-value threshold. **E** Boxplots showing Tumor Mutational Burden (TMB), as number of mutations per megabases, distribution comparing either GEP-NENs and MTCs (left panel) or NETs and NECs (right panel). T-test p-values are shown on the top

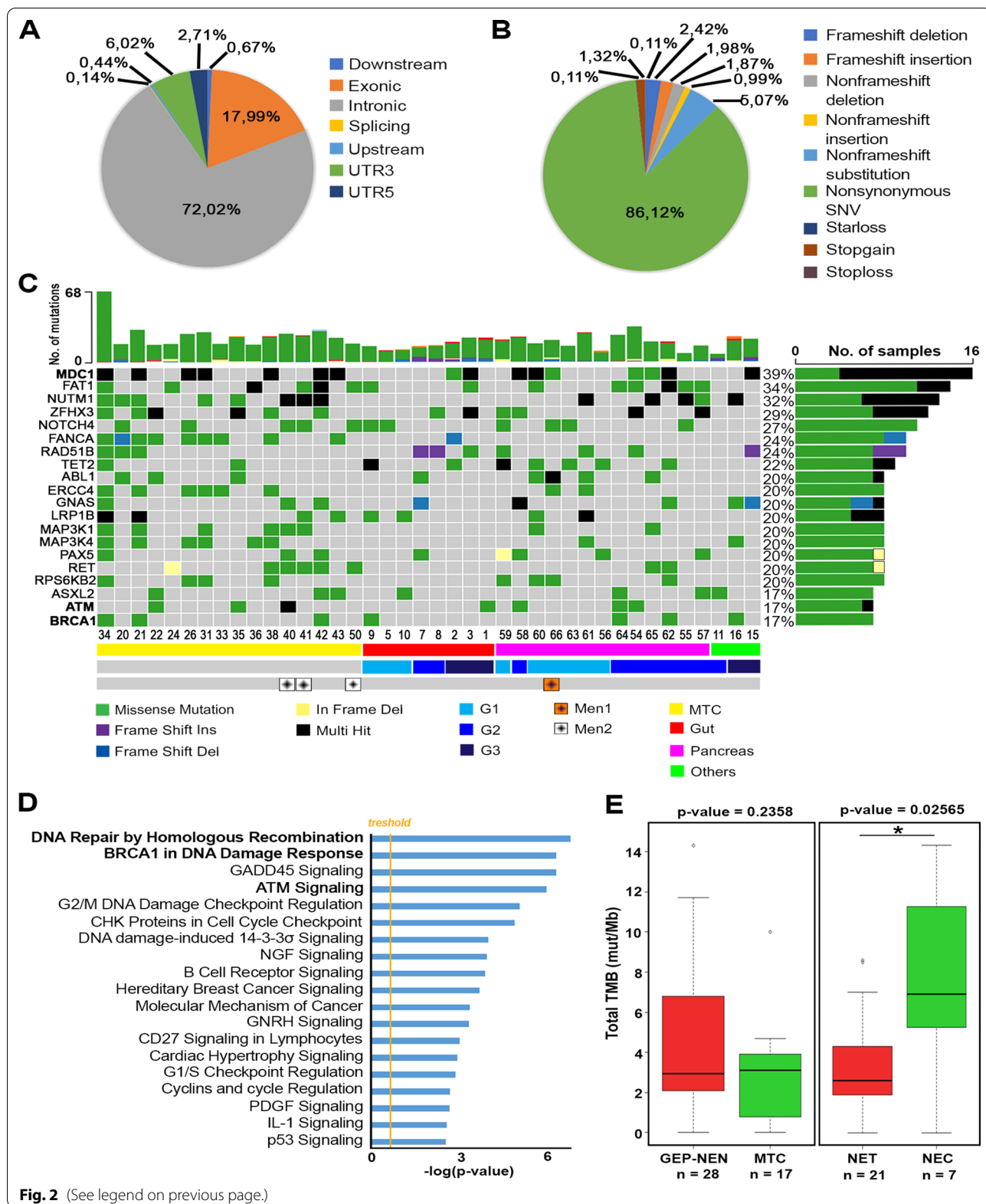


**Fig. 2** (See legend on previous page.)

these are involved in pathways related to genome stability maintenance, such as DNA repair by homologous recombination, DNA damage response and checkpoint regulation and ATM signaling (Fig. 2D). Finally, analyzing TMB status considering GEP-NEN and MTC groups, the median value was around 3; when considering NETs and NECs separately, within the GEP-NEN group, the median value increased significantly in NECs, in some cases exceeding 10 that is the threshold value over which a subject is predicted to be responsive to immunotherapy (Fig. 2E). MSI quantitative score, instead, was not informative, in line with what observed by others (data not shown).

DNA from 30 out of the 44 above analyzed samples was also subjected to molecular karyotype by CGH array, to evaluate the presence of CNVs. At a first glance the intriguing result was that, while GEP-NENs in general presented multiple deletions/duplications and several mosaicisms, with chromosomes 5, 6, 7, 11, 18, 22 and X mainly affected, MTCs mostly showed single events per sample, except for one case, mostly representing deletions (Fig. 3A, B). From the previous analysis of the multigene panel test that allows the identification of gene amplifications, it emerged that EGFR and BRAF genes, both located on chromosome 7, were among the most frequently amplified in our GEP-NEN samples (Table 2). The most commonly amplified of all, RPS6KB1, is instead located on chromosome 17 that resulted duplicated only in few cases (Table 2 and Fig. 3B). As expected, MTC samples did not show gene amplification events.

Since total RNA was also sequenced by NGS for the same sample set as above, plus 20 more for which only RNA was available (Additional file 4: Table S3), data was analyzed to assess the concordance of gene expression data with the amplification/deletion patterns described and for the presence of fusion transcripts. Regarding the first point, significant correspondence between DNA rearrangements and gene counts was observed in most cases. This was relieved, among others, for chromosome 19, where patients harboring amplifications showed a trend to an overall increased gene counts within the same chromosome with respect to not amplified samples

(Fig. 3C), and for chromosome 22, in which an opposite scenario was observed for patients showing deletions (Fig. 3D). For the second point, according to the filtering criteria described in the methods and after discarding low quality samples (6 out of the 66 samples available), 20 fusion transcripts were detected. Most of them have been found only in 1 patient and few in 2 or 3 patients (Table 3, Fig. 3A). Interestingly, although MTC tissues were very little subject to the presence of fusion transcripts, confirming the low frequency of chromosomal rearrangement events in this type of neoplasm, the fusion AL391840.3-SH3BGRL2, previously identified in high-grade serous ovarian cancer [53], was retrieved in two MTC patients in our cohort (Table 3). Further experiments will be needed to investigate the functional significance of these rearrangements in NENs development and patients' survival.

### NEN miRNome profiling

To investigate miRNA expression profiles with the attempt to identify deregulated molecules useful as NEN biomarkers, smallRNA-Seq was performed (Additional file 5: Table S4), allowing the identification of 623 miRNAs commonly expressed in GEP-NENs and in MTCs (Fig. 4A).

Functional analysis on their target mRNAs, expressed in the investigated samples (Additional file 6: Table S5), revealed their involvement in pathways implicated in neurologic and endocrine cancers, such as glioblastoma multiforme, glioma and pancreatic adenocarcinoma signaling, together with others specifically involved in tumor development and progression, including epithelial adherens junctions, TGF- $\beta$ , PTEN and NGF signalings (Fig. 4B). Lacking either paired or independent normal tissues, it was not possible to identify differentially expressed coding and noncoding transcripts in cancer samples. Despite this, considering only GEP-NEN tissues, we evaluated the possible evidence of differentially expressed miRNAs among grades and this was indeed the case. How other research groups already hypothesized [54], a set of miRNAs, 52 in our case, were significantly

(See figure on next page.)

**Fig. 3** Genomic rearrangements of NENs. **A** Circos plot showing aCGH-derived genomic rearrangements (middle ring) and fusion transcripts (inner ring) retrieved among the analyzed samples. External colored ring indicates chromosomes. Red bars represent deletions, while green ones show amplifications. The grid behind the bars shows the number of samples presenting rearrangements. The thin lines in the bars represent the presence of only a part of the aberration in some samples. The curved lines in the inner ring indicate the fusion genes in their exact location. Gene names are shown on the outer ring. **B** Heatmap representing aCGH-derived genomic rearrangements in the 30 samples considered for analysis. Each row represents a chromosome while each column represents a patient whose numeric code is listed in the lower side. Shades of red and green indicate the rearrangement type as shown in the side legend. The bar with the different color blue shades represents tumor grades. **C** Boxplot representing gene counts between samples showing (green) or lacking (grey) amplification of chromosome 19. **D** Boxplot representing gene counts between samples having (red) or not (grey) deletion of chromosome 22



**Table 2** Gene amplifications

Gene	Samples (n)	Sample codes	Average fold change
RPS6KB1	12	1, 3, 5, 7, 8, 10, 11, 12, 15, 16, 55, 56	1.6
EGFR	9	2, 5, 8, 13, 15, 60, 61, 63, 65	1.6
BRAF	6	1, 5, 12, 13, 15, 61	1.5
ALK	4	5, 8, 10, 13	1.5
ERBB2	4	5, 12, 13, 55	1.9
FGF1	4	2, 4, 60, 61	1.6
FGFR1	4	2, 5, 13, 16	4.5
CCND3	3	2, 10, 16	1.5
CDK4	3	3, 61, 63	9.1
ERCC2	3	3, 5, 55	1.9
FGF10	3	3, 60, 61	1.7
FGF7	3	3, 15, 55	1.4
KIT	3	12, 13, 65	1.5
PDGFRA	3	5, 8, 12	1.5
RAF1	3	2, 5, 13	1.6
ERCC1	2	3, 5	2.0
FGF2	2	8, 12	1.5
LAMP1	2	5, 61	1.6
MET	2	13, 61	1.5
PDGFRB	2	60, 61	1.7
PIK3CA	2	5, 16	1.7
AR	1	3	1.5
BRCA2	1	2	1.4
CCND1	1	63	10.6
CDK6	1	61	1.6
ERBB3	1	63	2.8
FGF19	1	63	8.8
FGF23	1	3	1.5
FGF3	1	63	10.3
FGF4	1	63	10.3
FGFR2	1	5	2.1
FGFR4	1	61	1.9
JAK2	1	2	2.5
KRAS	1	3	1.4
MDM2	1	63	5.6
MDM4	1	15	1.5
MYC	1	3	26.5
MYCL	1	16	4.0
RICTOR	1	61	1.7
TFRC	1	5	3.1

differentially expressed between NETs and NECs and some of them also seemed to discriminate tumor grades (Additional file 7: Fig. S2). To identify possible circulating NENs biomarkers, smallRNA-Seq was performed on 3 patients for whom both tissues and serum samples were available; the same tissues underwent

**Table 3** Fusion transcripts

Fusion_name	Samples (n)	Samples code	Junction_Readcount
PMS2P11-AC105052.5	3	15, 57, 59	10_20_21
AL391840.3-SH3B-GRL2	2	27, 37	10_12
GDAP1-MIR2052HG	2	65, 66	10_15
MANEAL-ITFG1	2	15, 57	87_127
AC138035.1-SEPTIN14	1	65	16
BCAR3-ABCA4	1	13	17
CTPS2-GK	1	3	24
KHDRBS2_OT-KHDRBS2	1	57	17
LRMDA-KAT6B	1	13	12
MIA2-AL049828.1	1	61	11
MKRN1-BRAF	1	30	13
PMS2P9-AC105052.5	1	66	12
PPP1CB-BABAM2	1	13	11
PSMD3-AC015910.1	1	13	12
SMAD6-ZWILCH	1	13	57
SMBD1P-SDHAP1	1	39	11
TNS3-HUS1	1	13	38
TSPAN31-TEAD4	1	3	226
ZNF180-ERCC1	1	13	17
ZNF609-EYA2	1	13	72

multi omics analyses previously. This allowed the identification of 186 and 176 miRNAs respectively in two MTC sera and 232 in one pancreatic NET serum; from 94 to 98% of them was also expressed in the corresponding tissues (Additional file 5: Table S4). Then, a set of 13 miRNAs was selected for validation, taking into account the top100 expressed in the tissues analyzed, differentially expressed ones between NETs and NECs, as well as published evidences. The validation cohort was composed of both MTC and GEP-NEN patients; the former were further distinguished in either sporadic or hereditary (MEN1). Controls were globally matched for age and gender and, totally, 34 healthy controls and 42 patients were enrolled; among patients only 2 were G3 NENs, thus making not possible GEP-NEN grade stratification according to secreted miRNAs. Considering specifically the mRNAs targeted by the selected miRNA subset (Additional file 8: Table S6), these are implicated in ERK/MAPK, mTOR, HIF-1 $\alpha$ , p53 and ATM signal transduction pathways (Fig. 4C). Some of these pathways, in particular p53 and ATM, were resulted also affected by gene variants (Fig. 2D), thus suggesting a multi-level deregulation of such cascades during NENs development and progression. As shown in Fig. 4D, all the selected miRNAs resulted to be more highly

expressed in patients with respect to controls, most of them significantly discriminating between tumor affected and healthy subjects. On the other hand, grouping patients sera according to the origin of NEN, namely thyroid (MTC), pancreas sporadic (pNEN), pancreas familial (MEN1) or others (mostly including gut and lung NENs), it emerged that some miRNAs were significantly deregulated in specific subgroups. Specifically, miR143-3p was significantly upregulated in MEN1 and other NENs, miR144-3p and miR7-5p in MTC, miR335-5p in MTC and MEN1 and miR942-5p in MEN1. (Fig. 4E). Instead, miR-375 was significantly up-regulated in all the different subgroups and it was already proposed as circulating biomarkers in other cancer types [55]. However, this effect might be due to subgroups relative size and a larger case series would be needed to confirm the data.

#### Clinically actionable pathways prediction

In the investigated NENs, multi-omics analysis has revealed frequently mutated and duplicated genes, chromosome duplications/deletions, fusion transcripts and deregulated miRNAs. Altogether, considering this data, functional analysis was performed to highlight the most affected pathways that may be useful therapeutic targets in the treatment of these neoplasms. In details, considering the most frequently amplified genes in our dataset, PTEN signaling emerged among the most significantly affected (Fig. 5A) as already known especially for pancreatic NENs [11, 12]. In addition, the NGF signaling (Fig. 5B) known to be implicated in neuroendocrine neoplasms [56], includes some of the most frequently mutated genes in our casuistry. On the other hand, among deregulated miRNA targets, in Fig. 5C we reported those miRNAs significantly enrolled in HIF1 $\alpha$  signaling (Fig. 5C), known to be activated by RET in MTCs [57]. Considering, instead, the pathways impacted at different levels by gene alterations and miRNA deregulation, the well described p53 and the newly associated ATM signaling emerged among those significantly enriched, the former representing a potential novel therapeutic target in the treatment of this class of cancers. Indeed, the last network, showed in Fig. 5D, comprises deregulated

miRNA targets, mutated genes and, among them, MDM2 and MDM4 represent both downstream miRNA targets that have also been retrieved as amplified genes in some of the analyzed tissues, reinforcing the hypothesis of a possible multi-level targeting.

#### Discussion

NENs represent a heterogeneous group of neoplastic diseases originating from neuroendocrine cells distributed throughout the body. Conventionally, this cancer types are considered very difficult to diagnose due to the lack of molecular and prognostic markers and the difficulties in identifying the primary site of origin. Being mostly indolent, they are often already metastatic at diagnosis [3] and, indeed, selected NEN specimens are being included in clinical studies aiming at tumor origin identification [58]. Thus, the identification of early and specific diagnostic and prognostic markers as well as novel therapeutic targets is crucial. The current landscape of NENs genetic knowledge is heterogeneous, with well-defined traits by high-throughput studies for some anatomic sites such as pancreatic NENs, but relatively low information for other sites. Moreover, the increasing interest in circulating biomarkers offers a new perspective for earlier NENs diagnosis [59]. Furthermore, some studies have been conducted to emphasize the potential of miRNAs as biomarkers and for easier grade stratification and tissue discrimination in GEP-NENs [54, 60–62] and as promising diagnostic and prognostic factors in MTC [63–65].

In the present paper, a multi-omics approach has been applied to analyze a diversified NENs cohort composed of GEP-NENs and MTC primary tumors and few GEP-NEN derived metastasis. Given the heterogeneity of the cohort, with a small sample size for each group making it difficult to identify a histotype specific molecular signature, and considering the recently emerged concept that NENs from different organ systems inter-relate clinically and genetically [4], we focused on highlighting common molecular and functional features that might represent useful and effective NEN biomarkers and therapeutic targets.

The gene mutational landscape revealed, over the already known key drivers specifically associated with pancreatic NETs, pancreatic NECs [11, 66] and MTCs [6], a common signature represented by a set of genes

(See figure on next page.)

**Fig. 4** miRNA profiling in NENs tissue and serum. **A** Venn Diagram comparing MTC and GEP-NEN expressed miRNAs. **B** Dot plot of the most significant IPA canonical pathways involving commonly expressed miRNAs. Dot color ranges from red to purple depending on the  $-\log$  of the adjusted p-value. Dot sizes depend on the Gene Ratio as described in the figure. **C** GO-Plot showing some of the most important pathways involving the predicted target genes of miRNAs selected for validation. Different pathways are drawn with different colors. The pathway-involved target genes are reported in the outer ring. **D** Boxplots of the relative expression ( $2^{\Delta\text{-DDCT}}$ ) of each serum validated miRNA in NEN (blue) samples versus healthy controls (red). Asterisks indicate statistical significance ( $p$ -value  $< 0.05$ ). **E** Boxplots of the relative expression ( $2^{\Delta\text{-DDCT}}$ ) of each serum validated miRNA in different samples groups mentioned in the figure. The asterisks indicate statistical significance ( $p$ -value  $< 0.05$ )

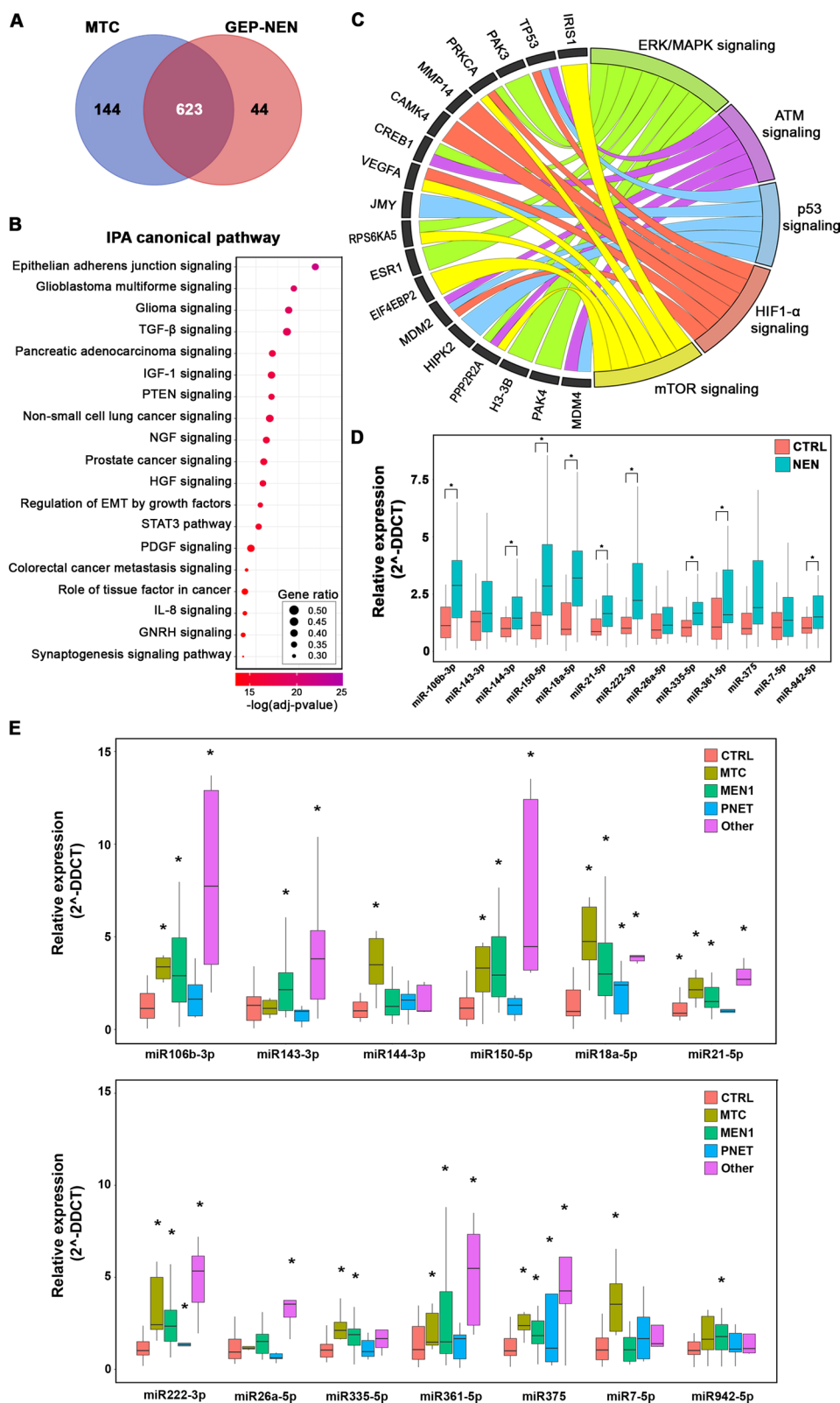
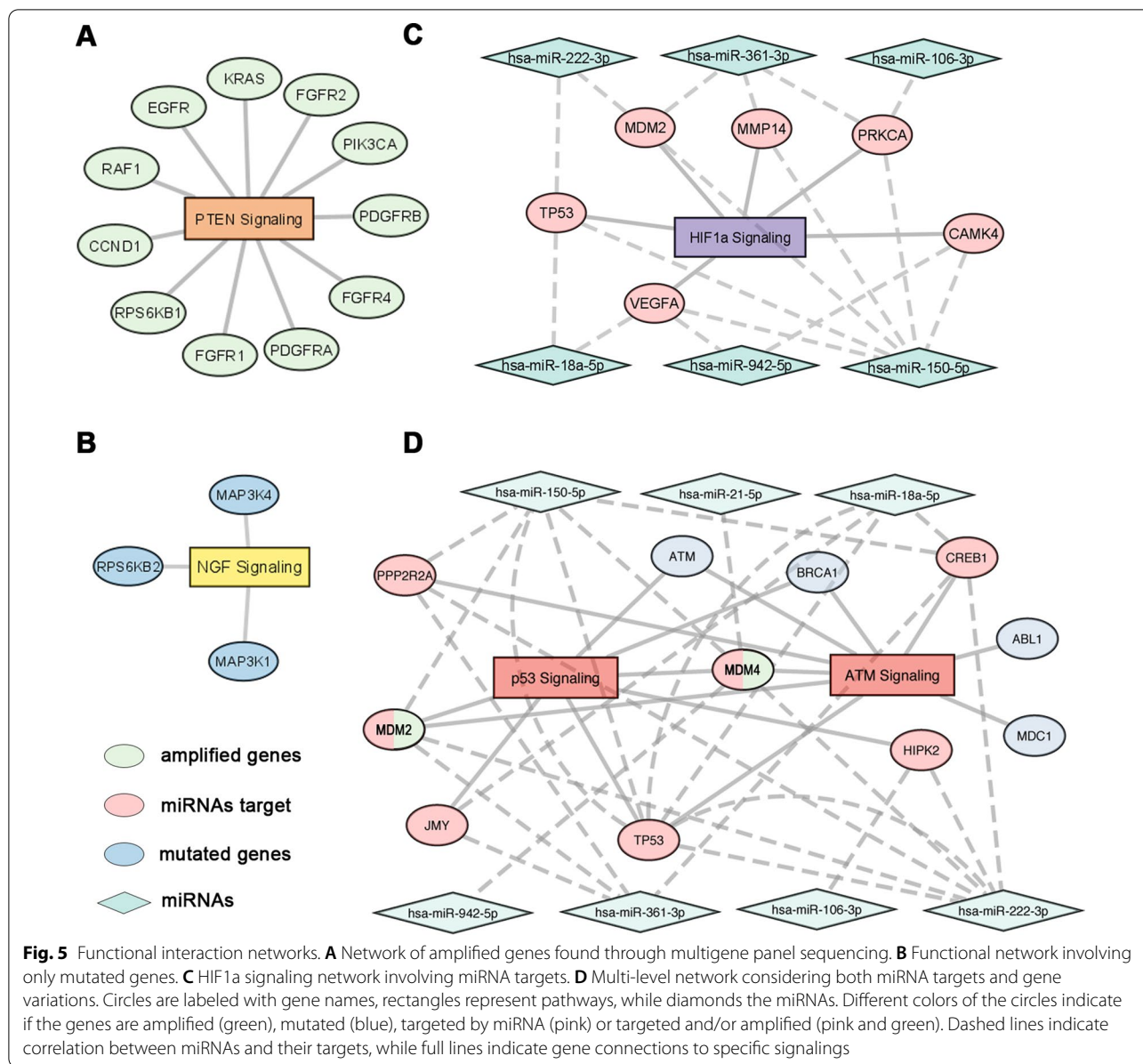


**Fig. 4** (See legend on previous page.)



most frequently mutated, among which those involved in genome stability maintenance and DNA damage recombination emerged, including MDC1, BRCA1 and ATM. In particular, MDC1 was never specifically associated to NENs before, except for one paper observing the presence of either MDC1 or ATM somatic mutations in RET and RAS negative MTCs [67]. In our cohort, instead, MDC1 resulted the top mutated gene in absolute among all NEN specimens analyzed. It is a key component of the DNA damage response, binding to  $\gamma$ -H2AX at DNA double-strand breaks, and participating in the recruitment of key factors including ATM, BRCA1, and TP53 [68]. MDC1 loss of function could negatively

affect both homologous recombination and non-homologous end joint repair pathways and co-mutation with some of its key co-factors has been proposed as potential marker for radiosensitivity [69]. Interestingly, within our cohort MDC1 resulted to be co-mutated with ATM in 2 out of 7 ATM-mutated samples and with BRCA1 in 4 out of 7 BRCA1-mutated ones. Moreover, we also found one ATM-BRCA co-mutation case (Fig. 2C). With these premises, not surprisingly, ATM signaling resulted among the most significantly impacted at gene level, together with other pathways involving BRCA and DNA repair, or enrolling ATM downstream targets such as G2/M and G1/S checkpoints and other DNA

damage-induced ones (Fig. 2D) [70]. On the other hand, complementary analyzes carried out on DNA and RNA samples, revealed a different behavior of GEP-NENs and MTCs regarding the tendency to form large chromosome rearrangements or gene amplifications and fusion transcripts. Indeed, as also observed before, GEP-NENs were more prone to this kind of events. Moreover, we observed a good concordance between the amplification/deletion patterns observed at chromosome level and gene expression data (Fig. 3). Given the absence of matched normal tissues, we did not sought to investigate differential expressed genes in tumor tissues except to have an indication of a possible deregulation among GEP-NENs of different grades even if this was not the main focus of the present work. As expected, several transcripts were found differentially expressed between grades, functionally targeting most of the pathways observed to be affected at the gene level, and, thereafter, post-transcriptionally through miRNA targeting (data not shown). Indeed, in the attempt to mainly focus on molecular features in common to the analyzed neoplasms, we proceeded by analyzing tissue miRNAs to identify those over-expressed in the various kind of investigated NENs. This led to the identification of a set of 623 commonly expressed miRNAs, with the top expressed being also mostly shared among different samples. Anyway, even in this case, a set of miRNAs resulted to be expressed at different level in low with respect to high-grade GEP-NENs, thus corroborating previous findings pointing to miRNAs as useful biomarkers for grade stratification in this class of NENs [54, 61]. In this context, considering our and others' evidence of high TMB in high-grade GEP-NENs and the proposed role for PDL1 expression in GEP-NENs grade stratification [71], a positive response of NETs-G3 and NECs to immunotherapy may be desirable and the impact of miRNA-mediated deregulation on PDL1 and other genes involved in the immunological synapse should be deeply investigated. In our case, although we observed PDL1 coding transcript over-expression in G3 vs G2 tumors, this appears not to be dependent on miRNA-mediated post-transcriptional regulation, although the limited number of high-grade tumors may have undermined the significance of the results (data not shown). Moreover, through a pilot sequencing by NGS of serum miRNAs from 3 patients, multiple miRNA molecules could be detected, with more than 95% of them being previously identified in the corresponding tissues. This finding reinforced the hypothesis that overexpressed miRNAs may be specifically released and evaluated as circulating NEN biomarkers.

Based on these results, we selected a set of 13 miRNAs to be evaluated in serum samples as possible circulating NEN biomarkers. We found that these miRNAs were overall significantly overexpressed in NEN patients compared to healthy subjects. This result represents a remarkable one, because for the first time a set of circulating miRNAs overexpressed in NENs patients could potentially represent a pathological signature for diagnostic purposes. A larger cohort with higher sample number for each histotype would be needed to confirm the data and select the most suitable molecule combination to be assessed for specific and reliable results.

Very interestingly, the mRNA targets of the selected miRNA panel are linked to ATM signaling (Fig. 4D) that we found emerging among the most significantly impacted at multiple levels (Fig. 5D). Taken together, we can speculate that ATM may represent a novel druggable pathway, in addition to the widely used inhibitors of mTOR [72–74], whose regulation by ATM has been also demonstrated [75, 76].

Indeed, following the success of PARP inhibitors, ATM inhibitors have been proposed in the therapeutic exploitation of DNA Damage Response (DDR) in cancer [77]. Several synthetic molecules have been already developed and demonstrated to induce significant sensitization to radiation and DNA-damaging chemotherapeutic agents [78], and some of them are undergoing clinical trials in combination with radiation therapy [79] or with PARP inhibitors [80].

In fact, according to an experimentally proven hypothesis, the use of an ATM inhibitor, shutting down the MDC1-mediated DDR pathway, together with PARP inhibitors, which rescue endogenous BIN1 expression (that increases cell death due to DNA damage), is able to generate a new 'BRCAness-independent' synthetic lethal effect in cancerous cells [81].

Taken together, our results reinforce this hypothesis, but further experimental and preclinical evidences are needed by establishing *in vitro* and *in vivo* models demonstrating their effectiveness and potential clinical application in NENs.

## Conclusions

The findings of the present study highlighted a novel molecular landscape of NENs, allowing the identification of a set of circulating miRNAs that may be investigated as NEN biomarkers, and suggesting ATM and its cofactors as possible molecular targets to be tested in combination with current therapies.

## Abbreviations

NEN: Neuroendocrine neoplasm; GEP-NEN: Gastroenteropancreatic neuroendocrine neoplasm; MTC: Medullary thyroid carcinoma; ATM: Ataxia Telangiectasia Mutated; MEN1: Multiple endocrine neoplasia type 1; MEN2: Multiple endocrine neoplasia type 2; VHL: Von Hippel–Lindau; NF1: Neurofibromatosis type 1; TSC: Tuberous sclerosis complex; WHO: World Health Organization; IARC: International Agency for Research on Cancer; NET: Neuroendocrine tumor; NEC: Neuroendocrine carcinoma; DAXX: Death Domain Associated Protein; ATRX: Alpha thalassemia/mental retardation syndrome X-linked; PTEN: Phosphatase and tensin homolog; TSC2: Tuberous sclerosis complex 2; mTOR: Mammalian target of rapamycin; MUTYH: MutY DNA glycosylase; CHEK2: Checkpoint Kinase 2; BRCA2: Breast Cancer gene 2; GI-NET: Gastrointestinal neuroendocrine tumor; CDKN1B: Cyclin dependent kinase inhibitor 1B; KRAS: Kirsten rat sarcoma virus; SMAD4: SMAD family member 4; TP53: Tumor Protein P53; BRCA1: Breast Cancer gene 1; RB1: Retinoblastoma-associated protein; RET: Ret proto-oncogene; RAS: Rat sarcoma virus; CgA: Chromogranin A; Syn: Synaptophysin; 5-HIAA: 5-Hydroxyindoleacetic acid; NSE: Neuron-specific enolase; CD56: Cluster of differentiation 56; FFPE: Formalin fixed paraffin embedded; H&E: Hematoxylin and eosin; DIN: DNA integrity number; RIN: RNA integrity number; TMB: Tumor mutational burden; MSI: Microsatellite instability; IPA: Ingenuity pathway analysis; Ct: Cycle threshold; CGH: Comparative genomics hybridization; NGS: Next generation sequencing; SNV: Small nucleotide variant; CNV: Copy number variation; MDC1: Mediator of DNA damage checkpoint protein 1; DDR: DNA damage response; NUTM1: NUT midline carcinoma family member 1; ZFX3: Zinc finger homeobox 3; FAT1: FAT atypical cadherin 1; ERCC4: Excision repair cross-complementation group 4; MAP3K1: Mitogen-activated protein kinase kinase 1; MAP3K4: Mitogen-activated protein kinase kinase 4; RPS6KB2: Ribosomal protein S6 kinase beta-2; HRAS: HRas proto-oncogene; EGFR: Epidermal growth factor receptor; BRAF: B-Raf proto-oncogene; TGF- $\beta$ : Transforming growth factor beta; NGF: Nerve growth factor; ERK: Extracellular signal-regulated kinase; MAPK: Mitogen-activated protein kinase 1; HIF-1 $\alpha$ : Hypoxia inducible factor 1 subunit alpha; pNEN: Pancreas sporadic neuroendocrine neoplasm; MDM2: MDM2 proto-oncogene, E3 ubiquitin protein ligase; MDM4: Mdm2-like P53-binding protein;  $\gamma$ -H2AX: H2A.X variant histone; PARP: Poly(ADP-ribose) polymerase 1.

## Supplementary Information

The online version contains supplementary material available at <https://doi.org/10.1186/s12967-022-03511-7>.

**Additional file 1: Table S1.** Sample information.

**Additional file 2: Table S2.** TSO500 all variants.

**Additional file 3: Fig. S1.** Mutational profile of different NEN classes. (A) Oncoplot representation of the TOP 20 mutated genes in MTC samples. The gray bar in the bottom figure highlights the presence of familiar syndrome MEN2. (B) Oncoplot representation of the TOP 20 mutated genes in GEP-NETs (G1 and G2 NENs). Gray bars at the bottom indicate the presence of familiar syndrome MEN1 (upper) and metastatic tissues (lower). (C) Oncoplot representation of the TOP 20 mutated genes in GEP-NEC. The bottom bar indicates metastases. In each graph each column represent a sample with its numeric code while each row represent a gene. Box colors refer to mutation type.

**Additional file 4: Table S3.** RNA-Seq all counts.

**Additional file 5: Table S4.** SmallRNA normalized counts.

**Additional file 6: Table S5.** Targets of common miRNAs.

**Additional file 7: Fig. S2.** Heatmap of Differentially Expressed miRNAs between GEP-NETs (G1 and G2) and GEP-NEC plus metastases (G3). The log transformed median for each group is shown.

**Additional file 8: Table S6.** Targets of miRNAs selected for validation.

## Acknowledgements

Not applicable.

## Author contributions

Conceptualization: RT and AW; samples collection: MV, CM, MC, ADM, FT, ST, RM, CP, AC; investigation: VM, AS, LP, MI, IDB, SC, VN; data analysis: DP, AG, GG; writing and original draft preparation VM, AS and RT; writing, review, and editing: FR, GN, MS, RT, and AW; funding acquisition: AW and RT. All authors read and approved the final manuscript.

## Funding

This study was supported by Regione Campania: 'La Campania lotta contro il cancro' project Rare-Plat-Net, CUP: B63D18000380007 and Progetto GENOMeSALUTE (POR Campania FESR 2014/2020, azione 1.5; CUP: B41C17000080007); Italian Association for Cancer Research (Grant Number IG-23068); University of Salerno (Fondi FARB 2019; CUP: ORSA195102) and Ministero dell'Istruzione, Università e Ricerca, (Progr. POC R&I 2014-2020 'Dottorati innovativi con caratterizzazione industriale' XXXV Ciclo (Fellowships DOT1328517, CUP D52G19000580006 to V.M.). V.M. is a PhD Student of the Doctorate in Translational Medicine for Development and Active Ageing of the University of Salerno. A.S. is a resident of the Postgraduate School in Clinical Pathology and Clinical Biochemistry of the University of Salerno.

## Availability of data and materials

The datasets supporting the findings of this study are available from the corresponding author upon reasonable request. The Raw sequencing data have been deposited in the EBI ArrayExpress database (<http://www.ebi.ac.uk/arrayexpress>) with the following accession numbers: E-MTAB-11529 for multigene panel sequencing; E-MTAB-11599 for RNA-Seq and E-MTAB-11598 for smallRNA-Seq data.

## Declarations

### Ethics approval and consent to participate

The study was performed in accordance with the Declaration of Helsinki. All patients provided written informed consent for the use of tumor samples, according to the institutional regulations and the study was approved by the ethics committee of the National Cancer Institute "G. Pascale" (Project name: "Fighting Cancer resistance: Multidisciplinary integrated Platform for a technological Innovative Approach to Oncotherapies (Campania Oncotherapies)"—Ethical approval no. 40/19 OSS—Date 2019 November 21) and by the ethical committee of Federico II University of Naples (Project name: Innovazioni diagnostiche e terapeutiche per tumori neuroendocrini, endocrini e per il glioblastoma—Ethical approval no. 223/19—Date 2019 July 16).

### Consent for publication

Not applicable.

### Competing interests

The authors declare that they have no competing interests.

### Author details

<sup>1</sup>Laboratory of Molecular Medicine and Genomics, Department of Medicine, Surgery and Dentistry "Scuola Medica Salernitana", University of Salerno, via S. Allende, 84081 Baronissi, SA, Italy. <sup>2</sup>Medical Genomics Program and Division of Oncology, AOU 'S. Giovanni di Dio e Ruggi d'Aragona' University of Salerno, Rete Oncologica Campana, 84131 Salerno, Italy. <sup>3</sup>Genome Research Center for Health, 84081 Baronissi, SA, Italy. <sup>4</sup>IRCCS Synlab SDN s.p.a, Via Gianturco 113, 80143 Naples, Italy. <sup>5</sup>Department of Medicine, Surgery and Dentistry "Scuola Medica Salernitana", University of Salerno, 84081 Baronissi, SA, Italy. <sup>6</sup>Endocrinology Unit, Department of Medicine (DIMED), University of Padua, Padua, Italy. <sup>7</sup>MeriGen Diagnostic & c sas, traversa M. Pietravalle 11, 80131 Naples, Italy. <sup>8</sup>Pathology Unit, Istituto Nazionale Tumori-IRCCS-Fondazione G. Pascale, Via Mariano Semmola, 80131 Naples, Italy. <sup>9</sup>Sarcomas and Rare Tumors Unit, Istituto Nazionale Tumori-IRCCS-Fondazione G. Pascale, Via Mariano Semmola, 80131 Naples, Italy. <sup>10</sup>Department of Clinical Medicine and Surgery, Endocrinology Unit, Federico II University, Naples, Italy. <sup>11</sup>UNESCO Chair for Health Education and Sustainable Development, Federico II University, Naples, Italy.

Received: 20 May 2022 Accepted: 28 June 2022  
Published online: 06 July 2022

## References

- Oronsky B, Ma PC, Morgensztern D, Carter CA. Nothing but NET: a review of neuroendocrine tumors and carcinomas. *Neoplasia*. 2017;19(12):991–1002.
- Maharjan CK, Ear PH, Tran CG, Howe JR, Chandrasekharan C, Quelle DE. Pancreatic neuroendocrine tumors: molecular mechanisms and therapeutic targets. *Cancers*. 2021. <https://doi.org/10.3390/cancers13205117>.
- Yao JC, Hassan M, Phan A, Dagohoy C, Leary C, Mares JE, et al. One hundred years after "carcinoid": epidemiology of and prognostic factors for neuroendocrine tumors in 35,825 cases in the United States. *J Clin Oncol*. 2008;26(18):3063–72.
- Rindi G, Klimstra DS, Abedi-Ardekani B, Asa SL, Bosman FT, Brambilla E, et al. A common classification framework for neuroendocrine neoplasms: an International Agency for Research on Cancer (IARC) and World Health Organization (WHO) expert consensus proposal. *Mod Pathol*. 2018;31(12):1770–86.
- Anlauf M, Garbrecht N, Bauersfeld J, Schmitt A, Henopp T, Komminoth P, et al. Hereditary neuroendocrine tumors of the gastroenteropancreatic system. *Virchows Arch*. 2007;451(Suppl 1):S29–38.
- Ciampi R, Romei C, Ramone T, Prete A, Tacito A, Cappagli V, et al. Genetic landscape of somatic mutations in a large cohort of sporadic medullary thyroid carcinomas studied by next-generation targeted sequencing. *iScience*. 2019;20:324–36.
- Nagtegaal ID, Odze RD, Klimstra D, Paradis V, Rugge M, Schirmacher P, et al. The 2019 WHO classification of tumours of the digestive system. *Histopathology*. 2020;76(2):182–8.
- Dabelić N, Kukić T, Fröbe A. Medullary thyroid cancer—feature review and update on systemic treatment. *Acta Clin Croat*. 2020;59(Suppl 1):50–9.
- Hadoux J, Pacini F, Tuttle RM, Schlumberger M. Management of advanced medullary thyroid cancer. *Lancet Diabetes Endocrinol*. 2016;4(1):64–71.
- Jiao Y, Shi C, Edil BH, de Wilde RF, Klimstra DS, Maitra A, et al. DAXX/ATRX, MEN1, and mTOR pathway genes are frequently altered in pancreatic neuroendocrine tumors. *Science*. 2011;331(6021):1199–203.
- Scarpa A, Chang DK, Nones K, Corbo V, Patch AM, Bailey P, et al. Whole-genome landscape of pancreatic neuroendocrine tumours. *Nature*. 2017;543(7643):65–71.
- Stevenson M, Lines KE, Thakker RV. Molecular genetic studies of pancreatic neuroendocrine tumors: new therapeutic approaches. *Endocrinol Metab Clin North Am*. 2018;47(3):525–48.
- Francis JM, Kiezun A, Ramos AH, Serra S, Pedamallu CS, Qian ZR, et al. Somatic mutation of CDKN1B in small intestine neuroendocrine tumors. *Nat Genet*. 2013;45(12):1483–6.
- Banck MS, Kanwar R, Kulkarni AA, Boora GK, Metge F, Kipp BR, et al. The genomic landscape of small intestine neuroendocrine tumors. *J Clin Invest*. 2013;123(6):2502–8.
- Saghaeiannajad Esfahani H, Vela CM, Chauhan A. Prevalence of TP-53/Rb-1 co-mutation in large cell neuroendocrine carcinoma. *Front Oncol*. 2021;11: 653153.
- Jesinghaus M, Konukiewicz B, Keller G, Kloor M, Steiger K, Reiche M, et al. Colorectal mixed adenoneuroendocrine carcinomas and neuroendocrine carcinomas are genetically closely related to colorectal adenocarcinomas. *Mod Pathol*. 2017;30(4):610–9.
- Cha YJ, Koo JS. Next-generation sequencing in thyroid cancer. *J Transl Med*. 2016;14(1):322.
- Cives M, Strosberg JR. Gastroenteropancreatic neuroendocrine tumors. *CA Cancer J Clin*. 2018;68(6):471–87.
- Dasari A, Shen C, Halperin D, Zhao B, Zhou S, Xu Y, et al. Trends in the incidence, prevalence, and survival outcomes in patients with neuroendocrine tumors in the United States. *JAMA Oncol*. 2017;3(10):1335–42.
- Wang SC, Parekh JR, Zuraek MB, Venook AP, Bergsland EK, Warren RS, et al. Identification of unknown primary tumors in patients with neuroendocrine liver metastases. *Arch Surg*. 2010;145(3):276–80.
- De Divitiis C, von Arx C, Grimaldi AM, Cicala D, Tatangelo F, Arcella A, et al. Metronomic temozolomide as second line treatment for metastatic poorly differentiated pancreatic neuroendocrine carcinoma. *J Transl Med*. 2016;14(1):113.
- Bhattacharyya T, Gupta R, Kapoor R, Mittal BR, Kalra N. A systematic review of management of neuroendocrine tumors: an experience from a tertiary care centre from India. *Clin Cancer Invest J*. 2014. <https://doi.org/10.4103/2278-0513.138052>.
- Bartz-Kurycki MA, Oluwo OE, Morris-Wiseman LF. Medullary thyroid carcinoma: recent advances in identification, treatment, and prognosis. *Ther Adv Endocrinol Metab*. 2021;12:20420188211049612.
- Zatelli MC, Torta M, Leon A, Ambrosio MR, Gion M, Tomassetti P, et al. Chromogranin A as a marker of neuroendocrine neoplasia: an Italian Multicenter Study. *Endocr Relat Cancer*. 2007;14(2):473–82.
- Klimstra DS, Modlin IR, Coppola D, Lloyd RV, Suster S. The pathologic classification of neuroendocrine tumors: a review of nomenclature, grading, and staging systems. *Pancreas*. 2010;39(6):707–12.
- Wedin M, Mehta S, Angerås-Kraftling J, Wallin G, Daskalakis K. The role of serum 5-HIAA as a predictor of progression and an alternative to 24-h urine 5-HIAA in well-differentiated neuroendocrine neoplasms. *Biology*. 2021. <https://doi.org/10.3390/biology10020076>.
- Klimstra DS. Pathologic classification of neuroendocrine neoplasms. *Hematol Oncol Clin North Am*. 2016;30(1):1–19.
- Singh S, Asa SL, Dey C, Kennecke H, Laidley D, Law C, et al. Diagnosis and management of gastrointestinal neuroendocrine tumors: an evidence-based Canadian consensus. *Cancer Treat Rev*. 2016;47:32–45.
- Faggiano A, Lo Calzo F, Pizza G, Modica R, Colao A. The safety of available treatments options for neuroendocrine tumors. *Expert Opin Drug Saf*. 2017;16(10):1149–61.
- Faggiano A, Di Maio S, Mocerino C, Ottaviano M, De Divitiis C, Guarnotta V, et al. Therapeutic sequences in patients with grade 1–2 neuroendocrine tumors (NET): an observational multicenter study from the ELIOS group. *Endocrine*. 2019;66(2):417–24.
- Hinrichs AS, Karolchik D, Baertsch R, Barber GP, Bejerano G, Clawson H, et al. The UCSC genome browser database: update 2006. *Nucleic Acids Res*. 2006;34(Database issue):D590–8.
- Chang X, Wang K. wANNOVAR: annotating genetic variants for personal genomes via the web. *J Med Genet*. 2012;49(7):433–6.
- Mayakonda A, Lin DC, Assenov Y, Plass C, Koeffler HP. Maftools: efficient and comprehensive analysis of somatic variants in cancer. *Genome Res*. 2018;28(11):1747–56.
- Krzywinski M, Schein J, Birol I, Connors J, Gascoyne R, Horsman D, et al. Circo: an information aesthetic for comparative genomics. *Genome Res*. 2009;19(9):1639–45.
- Andrews S. FastQC: a quality control tool for high throughput sequence data. 2010.
- Martin M. Cutadapt removes adapter sequences from high-throughput sequencing reads. *EMBnet J*. 2011. <https://doi.org/10.14806/ej.17.1.200>.
- Dobin A, Davis CA, Schlesinger F, Drenkow J, Zaleski C, Jha S, et al. STAR: ultrafast universal RNA-seq aligner. *Bioinformatics*. 2013;29(1):15–21.
- Liao Y, Smyth GK, Shi W. featureCounts: an efficient general purpose program for assigning sequence reads to genomic features. *Bioinformatics*. 2014;30(7):923–30.
- Love MI, Huber W, Anders S. Moderated estimation of fold change and dispersion for RNA-seq data with DESeq2. *Genome Biol*. 2014;15(12):550.
- Haas BJ, Dobin A, Stransky N, Li B, Yang X, Tickle T, et al. STAR-fusion: fast and accurate fusion transcript detection from RNA-Seq. *bioRxiv*. 2017;34:533.
- Panero R, Rinaldi A, Memoli D, Nassa G, Ravo M, Rizzo F, et al. iSmaRT: a toolkit for a comprehensive analysis of small RNA-Seq data. *Bioinformatics*. 2017;33(24):4050.
- Sticht C, De La Torre C, Parveen A, Gretz N. miRWalk: an online resource for prediction of microRNA binding sites. *PLoS ONE*. 2018;13(10): e0206239.
- Walter W, Sánchez-Cabo F, Ricote M. GPlot: an R package for visually combining expression data with functional analysis. *Bioinformatics*. 2015;31(17):2912–4.
- Shannon P, Markiel A, Ozier O, Baliga NS, Wang JT, Ramage D, et al. Cytoscape: a software environment for integrated models of biomolecular interaction networks. *Genome Res*. 2003;13(11):2498–504.
- Lloyd R, Osamura R, Klöppel G, Rosai J. WHO classification of tumours of endocrine organs. Lyon: IARC Press; 2017.
- Klimstra D, Kloppell G, La Rosa S, Rindi G. Classification of neuroendocrine neoplasms of the digestive system. In: WHO Classification of Tumours Editorial Board, editor. WHO Classification of tumours: digestive system tumours. Lyon: International Agency for Research on Cancer; 2019. p. 16.
- Eriksson B, Oberg K, Stridsberg M. Tumor markers in neuroendocrine tumors. *Digestion*. 2000;62(Suppl 1):33–8.

48. Blind E, Schmidt-Gayk H, Sinn HP, O'Connor DT, Raue F. Chromogranin A as tumor marker in medullary thyroid carcinoma. *Thyroid*. 1992;2(1):5–10.
49. Ohmoto A, Sato Y, Asaka R, Fukuda N, Wang X, Urasaki T, et al. Clinicopathological and genomic features in patients with head and neck neuroendocrine carcinoma. *Mod Pathol*. 2021. <https://doi.org/10.1038/s41379-021-00869-9>.
50. Stewart GS, Wang B, Bignell CR, Taylor AM, Elledge SJ. MDC1 is a mediator of the mammalian DNA damage checkpoint. *Nature*. 2003;421(6926):961–6.
51. Nakanishi M, Ozaki T, Yamamoto H, Hanamoto T, Kikuchi H, Furuya K, et al. NFB1/MDC1 associates with p53 and regulates its function at the crossroad between cell survival and death in response to DNA damage. *J Biol Chem*. 2007;282(31):22993–3004.
52. Ruff SE, Logan SK, Garabedian MJ, Huang TT. Roles for MDC1 in cancer development and treatment. *DNA Repair*. 2020;95: 102948.
53. Newtonson A, Reyes H, Devor EJ, Goodheart MJ, Bosquet JG. Identification of novel fusion transcripts in high grade serous ovarian cancer. *Int J Mol Sci*. 2021. <https://doi.org/10.3390/ijms22094791>.
54. Cavalcanti E, Galleggiante V, Coletta S, Stasi E, Chieppa M, Armentano R, et al. Altered miRNAs expression correlates with gastroenteropancreatic neuroendocrine tumors grades. *Front Oncol*. 2020;10:1187.
55. Wu X, Somlo G, Yu Y, Palomares MR, Li AX, Zhou W, et al. De novo sequencing of circulating miRNAs identifies novel markers predicting clinical outcome of locally advanced breast cancer. *J Transl Med*. 2012;10:42.
56. Chen WY, Wen YC, Lin SR, Yeh HL, Jiang KC, Chen WH, et al. Nerve growth factor interacts with CHRM4 and promotes neuroendocrine differentiation of prostate cancer and castration resistance. *Commun Biol*. 2021;4(1):22.
57. Takacova M, Bullova P, Simko V, Skvarkova L, Poturnajova M, Feketeova L, et al. Expression pattern of carbonic anhydrase IX in medullary thyroid carcinoma supports a role for RET-mediated activation of the HIF pathway. *Am J Pathol*. 2014;184(4):953–65.
58. Sun W, Wu W, Wang Q, Yao Q, Feng Q, Wang Y, et al. Clinical validation of a 90-gene expression test for tumor tissue of origin diagnosis: a large-scale multicenter study of 1417 patients. *J Transl Med*. 2022;20(1):114.
59. Khan MS, Kirkwood A, Tsiganis T, Garcia-Hernandez J, Hartley JA, Caplin ME, et al. Circulating tumor cells as prognostic markers in neuroendocrine tumors. *J Clin Oncol*. 2013;31(3):365–72.
60. Li C, Zhou T, Chen J, Li R, Chen H, Luo S, et al. The role of Exosomal miRNAs in cancer. *J Transl Med*. 2022;20(1):6.
61. Panarelli N, Tyryshkin K, Wong JJM, Majewski A, Yang X, Scognamiglio T, et al. Evaluating gastroenteropancreatic neuroendocrine tumors through microRNA sequencing. *Endocr Relat Cancer*. 2019;26(1):47–57.
62. Colao A, de Nigris F, Modica R, Napoli C. Clinical epigenetics of neuroendocrine tumors: the road ahead. *Front Endocrinol*. 2020;11: 604341.
63. Chiacchiarini M, Trocchianesi S, Besharat ZM, Po A, Ferretti E. Role of tissue and circulating microRNAs and DNA as biomarkers in medullary thyroid cancer. *Pharmacol Ther*. 2021;219: 107708.
64. Romeo P, Colombo C, Granata R, Calareso G, Gualeni AV, Dugo M, et al. Circulating miR-375 as a novel prognostic marker for metastatic medullary thyroid cancer patients. *Endocr Relat Cancer*. 2018;25(3):217–31.
65. Shabani N, Razaviyan J, Paryan M, Tavangar SM, Azizi F, Mohammadi-Yeganeh S, et al. Evaluation of miRNAs expression in medullary thyroid carcinoma tissue samples: miR-34a and miR-144 as promising overexpressed markers in MTC. *Hum Pathol*. 2018;79:212–21.
66. Yan J, Yu S, Jia C, Li M, Chen J. Molecular subtyping in pancreatic neuroendocrine neoplasms: new insights into clinical, pathological unmet needs and challenges. *Biochim Biophys Acta Rev Cancer*. 2020;1874(1): 188367.
67. Agrawal N, Jiao Y, Sausen M, Leary R, Bettgowda C, Roberts NJ, et al. Exomic sequencing of medullary thyroid cancer reveals dominant and mutually exclusive oncogenic mutations in RET and RAS. *J Clin Endocrinol Metab*. 2013;98(2):E364–9.
68. Coster G, Goldberg M. The cellular response to DNA damage: a focus on MDC1 and its interacting proteins. *Nucleus*. 2010;1(2):166–78.
69. Kao J, Milano MT, Javaheri A, Garofalo MC, Chmura SJ, Weichselbaum RR, et al. gamma-H2AX as a therapeutic target for improving the efficacy of radiation therapy. *Curr Cancer Drug Targets*. 2006;6(3):197–205.
70. Menolfi D, Zha S. ATM, ATR and DNA-PKcs kinases—the lessons from the mouse models: inhibition ≠ deletion. *Cell Biosci*. 2020;10:8.
71. Cavalcanti E, Armentano R, Valentini AM, Chieppa M, Caruso ML. Role of PD-L1 expression as a biomarker for GEP neuroendocrine neoplasm grading. *Cell Death Dis*. 2017;8(8): e3004.
72. Okuyama H, Ikeda M, Okusaka T, Furukawa M, Ohkawa S, Hosokawa A, et al. A phase II trial of everolimus in patients with advanced pancreatic neuroendocrine carcinoma refractory or intolerant to platinum-containing chemotherapy (NECTOR trial). *Neuroendocrinology*. 2020;110(11–12):988–93.
73. Wolin E, Mita A, Mahipal A, Meyer T, Bendell J, Nemunaitis J, et al. A phase 2 study of an oral mTORC1/mTORC2 kinase inhibitor (CC-223) for non-pancreatic neuroendocrine tumors with or without carcinoid symptoms. *PLoS ONE*. 2019;14(9): e0221994.
74. Faggiano A, Malandrino P, Modica R, Agrimi D, Aversano M, Bassi V, et al. Efficacy and safety of everolimus in extrapancreatic neuroendocrine tumor: a comprehensive review of literature. *Oncologist*. 2016;21(7):875–86.
75. Cam H, Easton JB, High A, Houghton PJ. mTORC1 signaling under hypoxic conditions is controlled by ATM-dependent phosphorylation of HIF-1α. *Mol Cell*. 2010;40(4):509–20.
76. Alexander A, Cai SL, Kim J, Nanez A, Sahin M, MacLean KH, et al. ATM signals to TSC2 in the cytoplasm to regulate mTORC1 in response to ROS. *Proc Natl Acad Sci USA*. 2010;107(9):4153–8.
77. Choi W, Lee ES. Therapeutic targeting of DNA damage response in cancer. *Int J Mol Sci*. 2022. <https://doi.org/10.3390/ijms23031701>.
78. Durant ST, Zheng L, Wang Y, Chen K, Zhang L, Zhang T, et al. The brain-penetrant clinical ATM inhibitor AZD1390 radiosensitizes and improves survival of preclinical brain tumor models. *Sci Adv*. 2018;4(6):eaat1719.
79. Waqar SN, Robinson C, Olszanski AJ, Spira A, Hackmaster M, Lucas L, et al. Phase I trial of ATM inhibitor M3541 in combination with palliative radiotherapy in patients with solid tumors. *Invest New Drugs*. 2022. <https://doi.org/10.1007/s10637-022-01216-8>.
80. Pike KG, Barlaam B, Cadogan E, Campbell A, Chen Y, Colclough N, et al. The identification of potent, selective, and orally available inhibitors of ataxia telangiectasia mutated (ATM) kinase: the discovery of AZD0156 (8-{6-[3-(dimethylamino)propoxy]pyridin-3-yl}-3-methyl-1-(tetrahydro-2H-pyran-4-yl)-1,3-dihydro-2H-imidazo[4,5-c]quinolin-2-one). *J Med Chem*. 2018;61(9):3823–41.
81. Folk WP, Kumari A, Iwasaki T, Cassimere EK, Pyndiah S, Martin E, et al. New synthetic lethality re-sensitizing platinum-refractory cancer cells to cisplatin in vitro: the rationale to co-use PARP and ATM inhibitors. *Int J Mol Sci*. 2021. <https://doi.org/10.3390/ijms222413324>.

## Publisher's Note

Springer Nature remains neutral with regard to jurisdictional claims in published maps and institutional affiliations.

Ready to submit your research? Choose BMC and benefit from:

- fast, convenient online submission
- thorough peer review by experienced researchers in your field
- rapid publication on acceptance
- support for research data, including large and complex data types
- gold Open Access which fosters wider collaboration and increased citations
- maximum visibility for your research: over 100M website views per year

At BMC, research is always in progress.

Learn more [biomedcentral.com/submissions](https://biomedcentral.com/submissions)

